LONGITUDINAL STABILITY OF FLAT BUNCHES WITH SPACE-CHARGE OR INDUCTIVE IMPEDANCE

I. Santiago González *, F. Zimmermann, CERN, Geneva, Switzerland

Abstract

We study the loss of Landau damping for the longitudinal plane via the "Sacherer formalism". Stability limits are calculated for several longitudinal beam distributions, in particular for two types of flat bunches, which could be of interest to the LHC upgrade. The resulting stability diagrams are computed and displayed for different azimuthal modes. A general recipe is given for calculating the threshold intensity in the case of a capacitive impedance below transition or, equivalently, for a purely inductive impedance above transition. The formalism was applied to the case of the PS Booster, as an example of space-charge impedance below transition, and to the SPS, as an example of inductive impedance above transition.

INTRODUCTION

The "large Piwinski angle" (LPA) scenario of the LHC upgrade [1] requires bunches of 5×10^{11} protons, spaced by 50 ns, with a flat longitudinal profile. For demonstrating the feasibility of such upgrade path, we must explore the stability of flat bunches. This paper extends earlier Landau-damping considerations [2, 3, 4] to longitudinally flat beams. More details can be found in Ref. [5].

DISPERSION RELATION

Following Sacherer [2] one can represent the beam particle distribution as the sum of a stationary component g_0 and a small perturbation g_1, $g(r,\theta,t) = g_0(r,\theta) + g_1(r,\theta,t)e^{-\imath\Omega t}$, with r and θ denoting (normalized) polar coordinates in the longitudinal phase space (where $r = 1$ refers to a maximum phase excursion $\pm\pi$, i.e. to a particle at the edge of the rf bucket). The function $g_1(r,\theta)$ is [2, 6]

$$g_1(r,\theta,t) = \sum_{m=1}^{\infty} R_m(r)e^{-\imath m\theta}e^{-\imath\Omega t} \ , \qquad (1)$$

where $R_m(r)$ designates a radial function for the m^{th} azimuthal mode, and Ω is the complex frequency whose imaginary part signals growth or Landau damping.

If the change in mode frequency induced by the impedance is small compared with the synchrotron frequency, the coupling between different azimuthal modes can be neglected, leading to the *Sacherer integral equation* for mode m:

$$(\Omega - m\omega_s(r))R_m(r) = \frac{dg_0}{dr}\int_0^{\infty} G_m(r,r')R_m(r')r'dr' \ . \qquad (2)$$

The variation of the angular synchrotron frequency ω_s with radial amplitude r gives rise to longitudinal Landau damping. Considering small amplitudes in a single rf system, we approximate this dependence as [2, 3, 4]

$$\omega_s(r) = (\omega_{s0} - Sr^2) \ , \qquad (3)$$

with r adopting values between 0 and 1 at the center and edge of the bunch, respectively, and ω_{s0} denoting the angular synchrotron frequency at the center of the bunch including the incoherent frequency shift with respect to the synchrotron frequency of a single particle ω_{s00}. The parameter S represents the total frequency spread inside the bunch.

The so-called *synthetic kernel* approach [7, 4] considers a simplified interaction where the functions G_m are of the form $G_m(r,r') \propto r^m r'^{m-1}$. This assumption reduces (2) to the *Sacherer dispersion relation* [2]

$$1 = \frac{\Delta\omega_m}{W_m}\int_0^{\infty} \frac{r^{2m}dg_0/dr}{\Omega - m\omega_{sc}(r)}\,dr \ . \qquad (4)$$

where $W_m = \int_0^{\infty} r^{2m}(dg_0/dr)dr$ is a normalization constant and $\Delta\omega_m$ the "dynamic coherent frequency shift", i.e. the frequency shift of the mth mode expected in the absence of longitudinal frequency spread. For a positive capacitive impedance below transition, or for an inductive impedance above transition, we have $\mathrm{Re}(\Delta\omega_m) > 0$.

FLAT BUNCHES

The Ruggiero-Berg radial phase-space distributions [8]

$$g(r) = \frac{n+1}{\pi\hat{\tau}^2}\left(1 - \frac{r^2}{\hat{\tau}^2}\right)^n \quad 0 < r < \hat{\tau} \ , \qquad (5)$$

depend on the parameter n. The corresponding spatial line densities [8, 5] are obtained via an Abel transform [10] as

$$\lambda(z) = \frac{n(n+1)\Gamma(n)}{\hat{\tau}\sqrt{\pi}\Gamma(n+\frac{3}{2})}\left(1 - \frac{z^2}{\hat{\tau}^2}\right)^{n+\frac{1}{2}} \qquad 0 < |z| < \hat{\tau} \ , \qquad (6)$$

where we can identify $\hat{\tau}$ as the half bunch length. For $n = 1/2$, the density (6) describes an 'elliptic' distribution, for $n = 1$ a 'parabolic' one, and for $n = 2$ a 'smooth' distribution first introduced by Sacherer [2]. It is interesting that also a 'flat' distributions can be obtained by letting the value of n approach the limit $-1/2$.

* on leave from University of the Basque Country, Bilbao, Spain

An alternative description of a flat distribution was suggested by M. Furman [9], who considered the line density

$$\lambda(z) = K(1 - |z/\hat{\tau}|^{1/p})^q \quad |z| < a, p, q \geq 0 \,, \qquad (7)$$

with K denoting a normalization constant. With $p = 0.039$ and $q = 10$, the distribution (7) yields a reasonable description of a flat bunch [9], which after normalization becomes

$$\lambda(z) = 0.5615/\hat{\tau}\left(1 - |z/\hat{\tau}|^{25}\right)^{10} \,. \qquad (8)$$

For this distribution the inverse Abel transformation [10],

$$g(r) = -\frac{1}{\pi}\int_r^\tau \frac{d\lambda(z)}{dz}\frac{dz}{\sqrt{z^2 - r^2}} \,, \qquad (9)$$

cannot easily be obtained analytically. However, its numerical computation is straightforward.

Examples of the Furman flat profile (7) and of various Berg-Ruggiero line densities (6), including the "flat" $n = -1/2$ case (more precisely, the distribution for $n = -0.49$ is displayed), along with the associated radial phase-space densities, are illustrated in Fig. 1 [5].

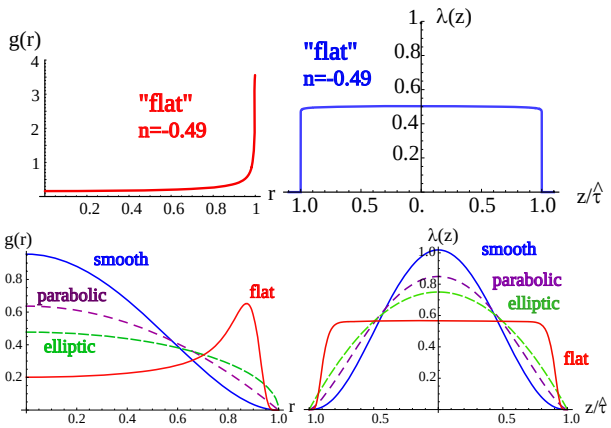

Figure 1: Radial phase space density (left) and longitudinal profile (right) for a flat distribution as limiting case of Ruggiero-Berg class of distributions (top) as well as for various other quasi-parabolic distribution functions and for another "flat" distribution à la M. Furman (bottom) [5].

STABILITY DIAGRAMS

The Sacherer dispersion relation (4) has an explicit analytic solution for the class of distributions given by (5). Namely, defining $z = (\omega_{sc0} - \Omega/m)/S$, for these distributions (4) becomes

$$1 = -\frac{\Delta\omega_m}{mS}\frac{\hat{\tau}^2}{z}{}_2F_1\left(1, 1+m; 1+m+n; \frac{\hat{\tau}^2}{z}\right) \,, \qquad (10)$$

where ${}_2F_1$ denotes the hypergeometric function.

For an arbitrary distribution g_0, we can transform (4) into

$$\frac{\Delta\omega_m}{mS}(z, m) = \frac{1}{F(z, m)} \,, \qquad (11)$$

with the function $F(z, m)$ defined as

$$F(z, m) \equiv \frac{\int_0^\infty u^m \frac{dg_0(u)/du}{u-z}du}{\int_0^\infty u^m (dg_0(u)/du)du} \,, \qquad (12)$$

where we have changed variables from r to $u \equiv r^2$.

The stability border can be visualized in the complex [Re($\Delta\omega_m$), Im($\Delta\omega_m$)] plane by drawing the complex coherent frequency shift $\Delta\omega_m$ obtained from (10) for z assuming real values between 0 and 1. An imaginary part of the frequency $\Delta\Omega$ equal zero (or real z) indicates that the perturbation neither damps nor grows, so that the corresponding tune shift $\Delta\omega_m$ lies on the border between stable and unstable motion.

Example stability diagrams for $n = 2$, 1, $1/2$, and $-1/2$ are presented in Figs. 2. With space charge below transition or with an inductive impedance above transition the coherent tune shifts towards the right with increasing beam intensity. Therefore, in these cases the instability threshold is related to $\Delta\omega_m/S(z)$ evaluated at $z = 0$.

Table 1 summarizes the coherent tune shift stability limits for various different distributions. For of Furman's flat distribution, the derivative of $g(r)$ — itself obtained via the numerical computation of (9) with $\lambda(z)$ taken from (8) — is calculated, again numerically, and plugged into the integral (12). We need to evaluate this integral only at $z = 0$ to obtain the threshold value for $\Delta\omega_m/S$.

Table 1 and Fig. 2 demonstrate that flat bunches in a single RF system are more stable than any of the considered types of non-flat bunches.

Table 1: Coherent tune shift stability thresholds of the lowest four modes for various longitudinal distributions normalized to the total synchrotron-frequency spread S [5]; $m = 1$ refers to the dipole mode, $m = 2$ to the quadrupolar one, etc.

distribution	n	$\frac{\Delta\omega_1}{S}$	$\frac{\Delta\omega_2}{S}$	$\frac{\Delta\omega_3}{S}$	$\frac{\Delta\omega_4}{S}$
smooth	2	0.33	1	1.8	2.67
parabolic	1	0.5	0.33	2.25	3.2
elliptic	1/2	0.67	1.6	2.57	3.56
flat	$-1/2$	2	2.67	3.6	4.57
flat (Furman)	N/A	1.58	2.13	2.90	3.71

INTENSITY THRESHOLDS

The coherent tune shift is proportional to the "effective" impedance and to the bunch population N_b [11], i.e.

$$\Delta\omega_m = C_m(\hat{\tau})\frac{N_b r_0 \eta c^3}{\gamma\omega_{s00}} i\left(\frac{Z}{n}\right)_{\text{eff}} \,, \qquad (13)$$

where η is the slippage factor, γ the relativistic Lorentz factor, c the speed of light, and r_0 the classical particle (here proton) radius. The function $C_m(\hat{\tau})$ depends on the mode

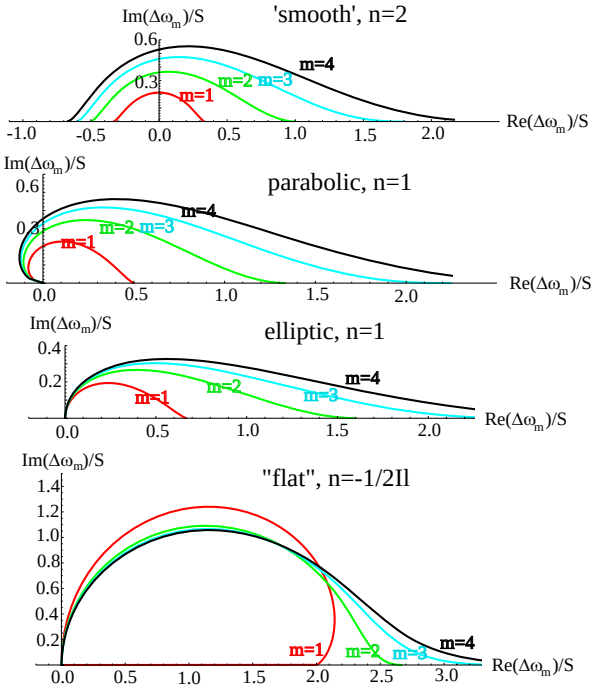

Figure 2: Stability diagrams computed from the Sacherer dispersion relation (4) in the complex tune shift plane, normalized to the bunch synchrotron frequency spread S, for Ruggiero-Berg distributions (5) with $n = 2$ ('smooth', top), $n = 1$ ('parabolic', second from top), $n = 1/2$ ('elliptic', third from top) and $n = -1/2$ ('flat', bottom), considering dipole ($m = 1$), quadrupolar ($m = 2$) and higher order modes of oscillation [5].

number m, on the bunch distribution and on the bunch length. For example, for a parabolic bunch one has [11] $C_m(\hat{\tau}) = 3/(4\pi^{3/2})\Gamma(m + 1/2)/(m - 1)!/\hat{\tau}^3$.

Through the relation (13) the threshold in $\Delta\omega_m/S$ can be converted into an intensity threshold.

CONCLUSIONS

Using the Sacherer formalism, we have derived, or rederived, the longitudinal instability thresholds for a pure space-charge impedance below transition, or an inductive impedance above transition. Different bunch distributions were considered. Our results suggest that in a single harmonic rf system longitudinally flat (or uniform) bunches are more stable than bunches of other, more typical shapes.

Stability diagrams are a useful tool from which approximate values of intensity thresholds can be obtained. The equivalent LHC bunch-intensity thresholds where longitudinal Landau damping is lost in the PS Booster ($Z_{\rm sc}/n \approx +i$ 5700 Ω) is about 8 times lower than the corresponding values for the SPS ($Z_{\rm ind}/n \approx -i$ 10 Ω), and even some 20–30% below the nominal bunch intensity [5]. In both these accelerators, the lowest thresholds are found for the dipole modes ($m = 1$), which are partially controlled by existing rf feedback loops.

Landau damping, if lost, can be restored by either increasing the frequency spread S, or by decreasing the frequency shift $\Delta\omega_m$, e.g. via flattening the bunch. Introducing a double rf system increases the frequency spread and could be a cure for loss of Landau damping. However, the double rf system is thought to create some other kind of instabilities [12]. Complicating matters, the non-linearities introduced by a double rf system do not permit any obvious simplification of the Sacherer equation in the same way as for a single harmonic system.

In the future we plan to study the implications of the "synthetic kernel" ansatz, to derive the function $C_m(\hat{\tau})$ for the different types of flat bunches, and to extend the formalism presented here to the case of multiple rf systems.

ACKNOWLEDGEMENTS

We thank G. Arduini, M. Chanel, A. Hofmann, E. Métral, K.Y. Ng, F. Pedersen, G. Rumolo, E. Shaposhnikova, and B. Zotter for helpful discussions and information. We acknowledge the support of the European Community-Research Infrastructure Initiative under the FP6 "Structuring the European Research Area" programme (CARE, contract number RII3-CT-2003-506395).

REFERENCES

[1] F. Zimmermann, "LHC Upgrade Scenarios," PAC2007, Albuquerque (2007).

[2] F.J. Sacherer, "A Longitudinal Stability Criterion for Bunched Beams," IEEE Tr. NS 20, 3, 825 (1973).

[3] E. Métral, "Longitudinal Bunched Beam Coherent Modes: From Stability to Instability and Inversely," CERN-AB-2004-002 (ABP).

[4] K.Y. Ng, "Comments on Landau Damping due to Synchrotron Frequency Spread," FERMILAB-FN-0762-AD (2005).

[5] I. Santiago González, "Loss of Longitudinal Landau Damping in the LHC Injectors," CERN-AB-Note-2008-001, CARE-NOTE-2007-012-HHH (2007).

[6] B. Zotter, "Longitudinal Stability of Bunched Beams Part II: Synchrotron Frequency Spread," CERN Report CERN SPS/81-19 (D1) (1981).

[7] F.J. Sacherer, "Methods for Computing Bunched Beam Instabilities," CERN report CERN/SI-BR/72-5, 1972

[8] F. Ruggiero, S. Berg, "Stability Diagrams for Landau Damping," Proc. PAC'97 Vancouver (1997).

[9] M.A. Furman, "E-Cloud in PS2, PS+, SPS+," Proc. LHC-LUMI-06 CERN-2007-002, CARE-Conf-07-004-HHH.

[10] P.W. Krempel, "The Abel-Type Integral Transformation and Its Application to Density Distributions of Particle Beams," MPS/Int.BR/74-1 (1974).

[11] A.W. Chao, Physics of Collective Beam Instabilities in High-Energy Accelerators, John Wiley, New York, 1993.

[12] E. Shaposhnikova et al, "Beam Transfer Functions and Beam Stabilisation in a Double RF System," PAC2005 Knoxville (2005).